

Pneumatically switchable graded index metamaterial lens

I. E. Khodasevych, I. V. Shadrivov, D. A. Powell, W. S. T. Rowe, and A. Mitchell

Citation: *Appl. Phys. Lett.* **102**, 031904 (2013); doi: 10.1063/1.4788918

View online: <http://dx.doi.org/10.1063/1.4788918>

View Table of Contents: <http://apl.aip.org/resource/1/APPLAB/v102/i3>

Published by the [AIP Publishing LLC](#).

Additional information on *Appl. Phys. Lett.*

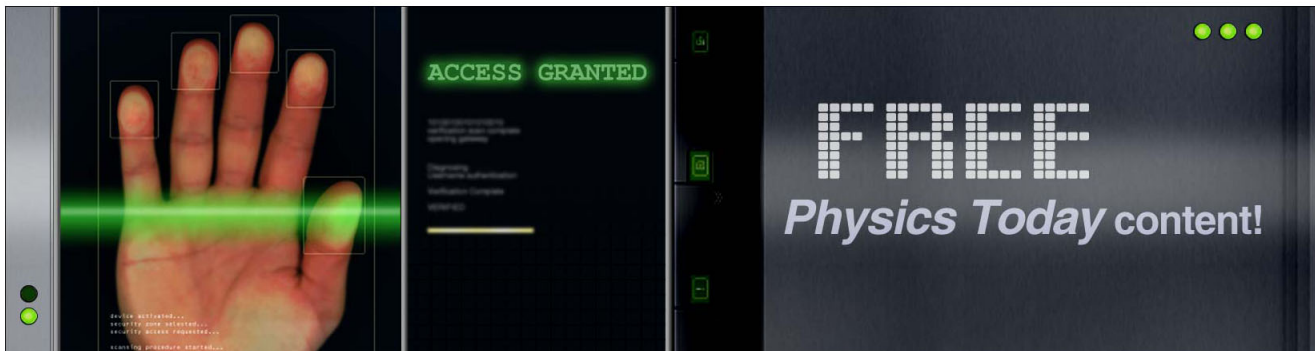
Journal Homepage: <http://apl.aip.org/>

Journal Information: http://apl.aip.org/about/about_the_journal

Top downloads: http://apl.aip.org/features/most_downloaded

Information for Authors: <http://apl.aip.org/authors>

ADVERTISEMENT



Pneumatically switchable graded index metamaterial lens

I. E. Khodasevych,^{1,2,a)} I. V. Shadrivov,³ D. A. Powell,^{2,3} W. S. T. Rowe,¹ and A. Mitchell^{1,2}

¹School of Electrical and Computer Engineering, RMIT University, Melbourne, VIC 3001, Australia

²ARC Centre for Ultrahigh bandwidth Devices for Optical Systems (CUDOS), Melbourne, VIC 3001, Australia

³Nonlinear Physics Centre, Research School of Physics and Engineering, Australian National University, Canberra, ACT 0200, Australia

(Received 2 September 2012; accepted 4 January 2013; published online 22 January 2013)

A low-profile pneumatically switchable graded index metamaterial lens operating at 9 GHz is proposed and practically demonstrated. An effective graded refractive index is engineered using an array of electric resonators of differing resonant frequency. Normal orientation of the resonators allows ultrathin single metamaterial layer lens design. Switching between focusing and non-focusing states is practically demonstrated by shorting the gaps in split ring resonators and eliminating the resonant response and the phase difference between the elements across the lens with pneumatically actuated metal patches that are pressed against the gaps of the resonators as the pressure in the chamber is reduced. © 2013 American Institute of Physics. [<http://dx.doi.org/10.1063/1.4788918>]

Graded refractive index lenses have uniform thickness and are considerably thinner than traditional curved lenses. However, the requirement to have varying refractive index within the material can pose a challenge for practical realization. The engineered refractive indices of metamaterials can be varied to a much greater extent than is possible with natural materials by adjusting the geometry of constituting unit cells.^{1–5} Also, exotic refractive properties, such as negative index, can be achieved. This could allow switching the lens from focusing (convex) to defocusing (concave). Metamaterial refraction is based on the resonant response of its unit cells. At frequencies close to the resonant frequency of the cell, the transmitted wave will experience a significant phase shift. By using unit cells of different geometry, and hence resonant frequency, the amount of phase shift through each element can be controlled, making it possible to create a parabolic phase profile required for lens operation.

Metamaterial graded index lenses exploiting magnetic resonators^{6,7} have been reported. These require the resonators to be oriented along the direction of propagation limiting the minimum thickness of the lens to the unit cell dimensions. Plasmonic lenses have also been demonstrated, but these too rely on thicknesses of the order of a wave length to achieve the required phase shifts.^{8–10}

Electrical resonators of split ring geometry^{11,12} should be oriented such that the E field of the incident radiation is directed across the gap in the center of the ring and the plane of the ring is normal to an incident plane wave. Such resonators enable planar, ultrathin designs, which are easy to fabricate using standard photolithography techniques. The thickness of a lens formed by such resonators will be limited by the thickness of the substrate used which can be an order of magnitude less than the unit cell size.

Tunable lenses can be valuable for many imaging applications. For radio frequency (RF) imaging, it may also be valuable to alter the electromagnetic signature of a lens when it is not in use for stealth purposes. Tunable lenses

have been achieved in traditional optics by moving a bulky combination of multiple lenses along the optical axis. More recently, tuning has been achieved using fluids¹³ and liquid crystal microlenses;¹⁴ however, these rely on the modest change in refractive index that is possible with these natural materials. A number of beam bending techniques have been proposed using plasmonic¹⁵ and metamaterial lenses,^{16,17} however, these were not tunable. Real time tuning of focal length was demonstrated in a plasmonic lens by heating it to high temperatures.¹⁸ Reconfiguring graded index of metamaterial via current induced heating of vanadium dioxide substrate was proposed.¹⁹ The exciting capability of operation in either focusing or defocusing states was demonstrated with a light-tunable metamaterial reflector, employing photo and light emitting diodes for continuous control.²⁰

In this work, we present a switchable metamaterial graded index lens. The lens switching is achieved using an array of pneumatically actuated metallic patches to short circuit the gaps in an array of split rings. The entire array can be actuated simultaneously and the pneumatic cell is electromagnetically transparent, hence it does not interfere with the operation of the lens.²¹

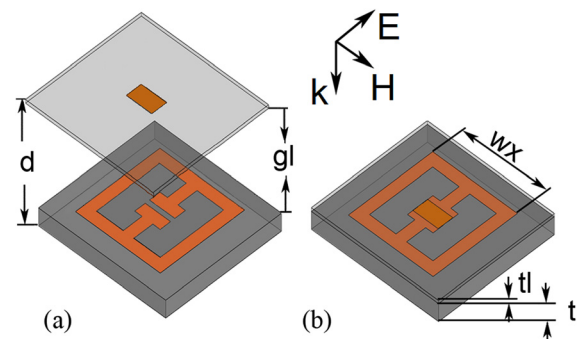


FIG. 1. Unit cell of the metamaterial lens with the following geometrical parameters: split ring resonator height $wy = 8$ mm, widths $wx = 6–10.5$ mm, trace width $wt = 1$ mm, gap $g = 0.4$ mm, gap length $lg = 2.4$ mm, RT/duroid 5880 ($\epsilon_r = 2.2$) thickness $t = 0.5$ mm, patches size 1×2.4 mm, on Ultralam 3850 ($\epsilon_r = 2.9$) of thickness $tl = 0.1$ mm, at distance $gl = 1$ mm from the split ring, unit cell dimensions 12×12 mm, total thickness $d = 1.6$ mm (a) open state ($gl = 1$ mm), (b) closed state ($gl = 0$ mm).

^{a)} Author to whom correspondence should be addressed. Electronic mail: iryna.khodasevych@student.rmit.edu.au.

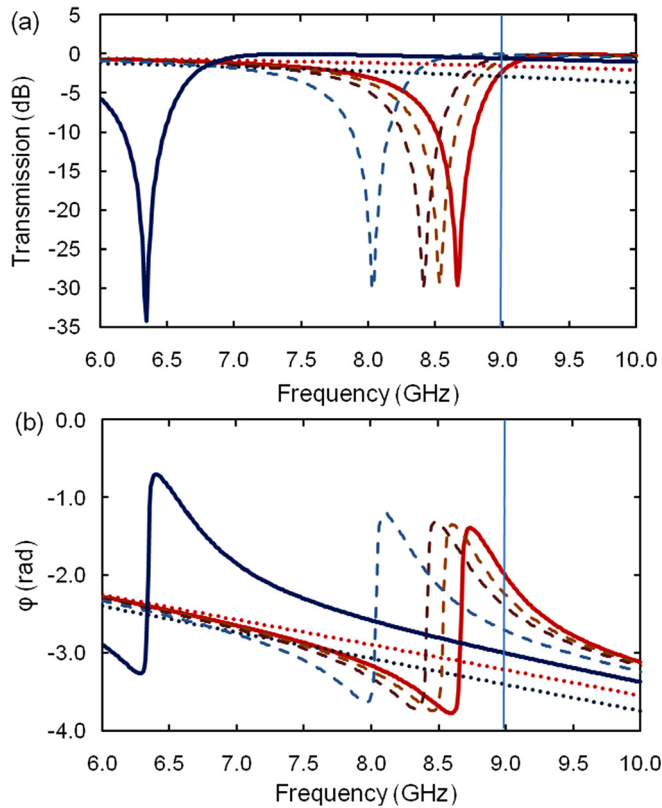


FIG. 2. (a) Transmission (b) phase shift through the split ring resonators with widths $w_x = 6$ mm (red solid line) and $w_x = 10.5$ mm (blue solid line) with height $w_y = 8$ mm. Dotted lines are for the same elements shorted with the metal patch. Dashed lines are for resonators with intermediate w_x values. The blue vertical line indicates the intended lens operation frequency.

The lens consists of a one dimensional array of copper split ring resonators on a Rogers RT/duroid substrate. The resonators are present only on one side of the substrate. Fig. 1 shows one of the resonators of this array. The polarization directions of the incident fields are indicated with arrows. Suspended above each split ring, on a flexible membrane, are additional copper patches. These can be pneumatically actuated to short circuit the gaps in split ring resonators.

In order to achieve focusing, a plane wave should experience a larger phase shift when travelling through the middle of the lens than the edges. The amount of phase shift through different parts of the lens can be engineered by adjusting the resonator geometries. We chose to adjust the width of each resonator. This width can be no larger than the width of the cell size of the array and can be no smaller than the gap feature in the centre of the resonator.

Fig. 2 depicts the transmission and phase shift through the equal height split ring resonators of the largest and the smallest widths. The resonant frequencies and phase shifts of elements with intermediate sizes fall in between these values and are shown in dashed lines. To obtain an accurate prediction of the resonator response, they were numerically simulated using ANSYS HFSS software; however, it was possible to estimate the required dimensions of the various resonators by approximating the response of each of these as similar to the central resonator but with frequency scaled by a factor proportional to the resonator loop length. The vertical line at 9 GHz depicts the most suitable frequency for lens operation. At 9 GHz, the transmission through the resonators is very

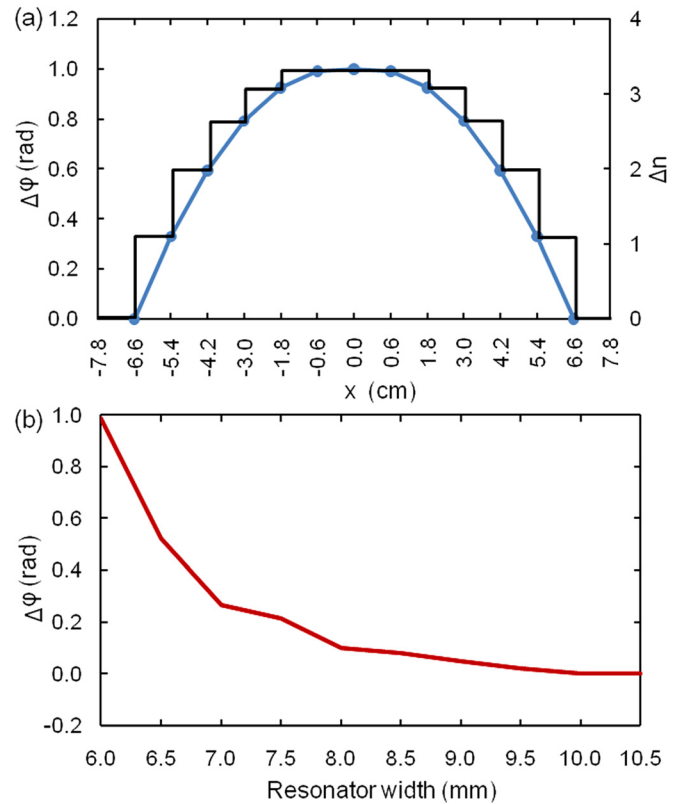


FIG. 3. (a) Parabolic phase and refractive index profile along the 15.6 cm length of the lens with staircase approximation. (b) Dependence of the phase shift on the split ring resonator width at the lens operation frequency of 9 GHz.

high, and the difference in transmission through elements of the largest and the smallest sizes does not exceed 3 dB. The maximum phase difference between the elements at this frequency is 1 rad. We also explored changing the height as well as the width of the resonator. This resulted in larger phase difference between the largest and the smallest elements. However, there were significant differences in transmission levels, making this approach unsuitable.

The dotted lines in Fig. 2 show the simulated transmission and phase shift through the same elements when the gaps are short circuited (as shown in Fig. 1(b)). The characteristic resonances in both phase and amplitude have been essentially eliminated in the 6–10 GHz range; however, a small amount of phase difference is still present due to different sizes of the elements. Transmission through the short circuited resonators is 2–3 dB lower than in the open state.

The required phase shift as a function of the lens width can be calculated from the equal optical length principle

$$\Delta\varphi = 2\pi(f - \sqrt{x^2 + f^2})/\lambda + \varphi_0, \quad (1)$$

where f is the focal length, λ is the wavelength, φ_0 is the phase shift at the centre of the lens, and x is the distance from the center of the lens. Since the maximum achievable phase difference between elements is 1 rad (φ_0), the focal length and the width of the lens were selected to fit the measurement window of 35×35 cm. This resulted in a 13 cell design which was 15.6 cm wide. Only one metamaterial layer in the direction of propagation was used. The thickness

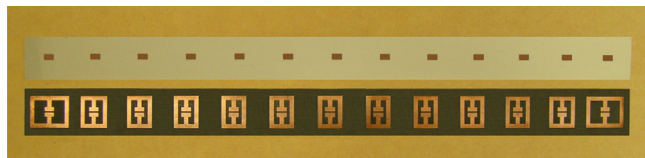


FIG. 4. Photograph of the layers before assembly.

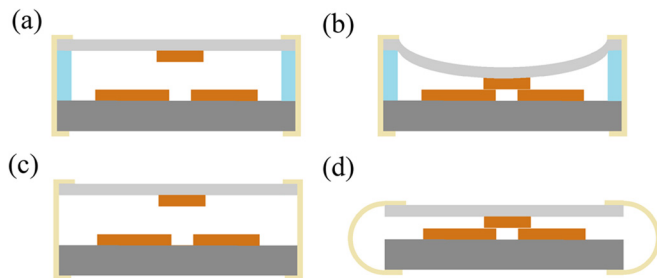


FIG. 5. Side view of framed (a) and (b) and unframed (c) and (d) assembly options in open (a) and (c) and closed (b) and (d) states.

of the lens was only 0.015λ . Addition of the pneumatic switching mechanism increased the thickness to 0.048λ , which is considerably less than previous metamaterial and plasmonic lenses. The equivalent relative refractive index of the lens as a function of position has been calculated from the relative phase shift using

$$\Delta n = (\Delta\phi/d)(\lambda/2\pi) \quad (2)$$

and assuming the material thickness d is the thickness of the physical structure. Fig. 3(a) shows the required parabolic phase profile and refractive index variation along the length of the lens calculated using Eqs. (1) and (2). Each step of this discrete staircase profile corresponds to a resonator cell. The relative phase shift as a function of resonator width is presented in Fig. 3(b), which was acquired from simulations as in Fig. 2(b) by referencing phase shift such that the element with least phase shift provides 0 rad. Using Figs. 3(a) and 3(b), the required width for each resonator in the array can be selected.

The lens was fabricated using standard printed circuit board photolithographic techniques. The resonator array was realized on Rogers RT/duroid 5880, while the shorting patches were realized on much thinner Rogers Ultralam 3858. Fig. 4 shows the fabricated layers of the lens. In order to assemble the lens, the layers were aligned so that metal patches were located over the gaps of split ring resonators and sealed around the edges of the lens using adhesive tape.

To ensure uniform distance between the layers, a 1 mm thick acrylic frame was used as a spacer around the perimeter of the lens as illustrated in Fig. 5(a). In the switch open position, the 1 mm distance was chosen to ensure that layer with the shortening patches is far enough from the split ring to minimize the coupling effect on the ring's resonant frequency and thus make structure more tolerant to variations in layer spacing. An outlet tube of 3 mm diameter was connected to one corner of the lens and led to a vacuum pump for pneumatic switching.

A prototype was also realized with the frame removed as illustrated in Fig. 5(c). This results in different shorting membrane behavior in the closed state. Figs. 5(b) and 5(d)

illustrate the side view of the lens with the vacuum applied to the framed and unframed versions. Although the frame ensures better control over the layer spacing, in this case, the membrane with patches has to be fairly flexible in order to bend into the structure. Also, the shorting elements have to be located along the middle of the membrane since this is the only part of the membrane that comes into contact with the bottom layer. With the frame removed, the top layer is not required to be flexible any more since the operation relies on the flexibility of the bonding tape acting as the flexible element. The entire surface area of the top layer comes into contact with the bottom layer allowing more versatile choice of resonator gap and patch positions.

As an initial test, the response of a single cell of the lens was measured with a free-space transmission system by masking the other cells with a metal plate. The pneumatic cavity was then evacuated and the response was again measured. It was found that an internal pressure of 0.2 bar was sufficient to eliminate the resonant features indicating effective shorting of the rings in the lens array.

The focal length of the lens obtained from Eq. (1) was 41 cm; however, at a width of 4.68λ and numerical aperture $NA = 0.32$; diffraction effects are expected to be significant. As suggested in the literature,^{18,22} for lenses of such small numerical aperture, the focal point is expected to be up to 75% shorter than predicted by simple geometrical optics.

Thus, in order to accurately predict the behavior of the lens, the whole structure was simulated using ANSYS HFSS software based on the full-wave finite element method. Figs. 6(a) and 6(b) show the simulated field intensity distributions of the lens in open and shorted positions, respectively, in response to a normally incident plane wave at 9 GHz. Focusing is seen at approximately 10 cm from the lens in the open state. No focusing is seen when the lens is shorted.

To experimentally measure the behavior of the physical lens, we used a parallel plate waveguide configuration with a scanning probe on the top plate.²³ A parabolic reflector was designed to convert the point source excitation into a plane wave incident normal to the lens, with electric field oriented across the gaps of the resonators. Initially static representations of the open and shorted states of the lens were measured.²⁴ The lens was then connected to a vacuum pump for real time switching. The field distributions for both open and shorted states were measured and compared to numerical simulations. Both framed and unframed versions of the lens were tested.

Figs. 6(c) and 6(d) present the measured field intensity distributions in open and short positions for the framed version and Figs. 6(e) and 6(f) are for the unframed version. Measured results for both versions of the lens are in good agreement with simulated results with focusing at around 10 cm at 9 GHz. Some inhomogeneity could be attributed to the deviation of the incident angle from the normal incidence, inhomogeneity of the layer spacing or layer displacement. Potentially useful operating regimes identified at other frequencies are presented in supplementary material (Fig. S1).²⁵

When the pneumatic pump was engaged and disengaged, the lens switched reversibly between shorted and open states without any noticeable change in performance.

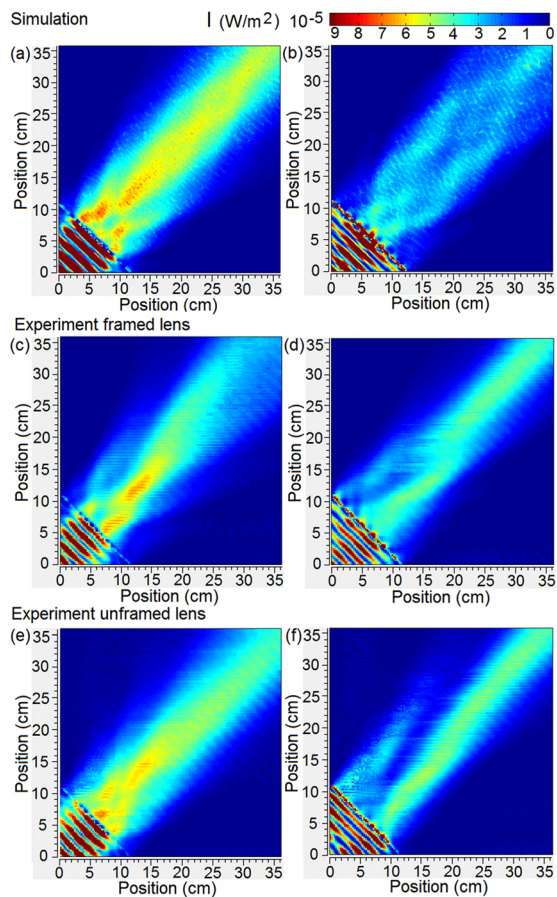


FIG. 6. Simulated (a) and (b) and measured (c)-(f) field intensity distributions for framed (c) and (d) and unframed (e) and (f) versions of the lens in open ($gl = 1$ mm, focusing) (a), (c), and (e) and shorted ($gl = 0$ mm, not focusing) (b), (d), and (f) states.

As future work, it may be possible to achieve a full π phase shift by stacking three resonator layers. This could enable the construction of a Fresnel zone plate configuration. The focal spot size could be reduced via an increase of the lens aperture; however, to maintain a parabolic phase profile, this would require an increase in the phase shift provided by the resonators at the center of the lens. We do not believe that a significant increase in phase shift could be achieved by improving the design of these resonators; however, such an increase may be possible by stacking resonators. The concept could be extended to two dimensional structures by placing resonators in a circular arrangement. Also polarization independent lenses could be designed by using polarization independent variations of split ring resonators with symmetrically located gaps.

By employing split ring resonators with multiple gaps, switching between various focal lengths and operation frequencies could be achieved. In this case, it would be possible to have identically sized resonant elements and reconfigure the lens by independently actuating the short circuits on each cell. With more precise control of air pressure in the chamber, continuous tuning of the focal length could be possible when, by gradually changing the pressure, one would control the distance between the patch and the split ring resonator gap, thus changing the capacitance and the resonant frequency of the resonators. Further, if a leak free valve was

introduced at the pneumatic port, the lens could be set to maintain either open or shorted state without requiring external power.

In conclusion, a pneumatically switchable graded index metamaterial lens operating at GHz frequencies has been designed, fabricated, and characterized. Split ring resonators of different widths, and hence resonant frequencies, were used to achieve the graded effective refractive index. By exploiting the electric resonance of split rings, an ultrathin lens of only 0.015λ was achieved. An experimental demonstration of switching between focused and unfocused states of the lens using pneumatically actuated metal patches was presented. On application of negative pressure, the metal patches were pressed against and short circuited the gaps in split ring resonators to eliminate the resonant response and corresponding phase difference between the elements at the edges and in the center of the lens. Two actuation structures were tested, both showing good agreement with the predicted behavior. A number of tuning possibilities were discussed and avenues for future work were identified.

- ¹D. R. Smith, J. J. Mock, A. F. Starr, and D. Schurig, *Phys. Rev. E* **71**, 036609 (2005).
- ²Y. Zhang, R. Mittra, and W. Hong, *J. Electromagn. Waves Appl.* **25**, 2178 (2011).
- ³J. Neu, B. Krolla, O. Paul, B. Reinhard, R. Beigang, and M. Rahm, *Opt. Express* **18**, 27748 (2010).
- ⁴R. Liu, Q. Cheng, J. Y. Chin, J. J. Mock, T. J. Cui, and D. R. Smith, *Opt. Express* **17**, 21030 (2009).
- ⁵Y. L. Loo, Y. Yang, N. Wang, Y. G. Ma, and C. K. Ong, *J. Opt. Soc. Am. A* **29**, 426 (2012).
- ⁶T. Driscoll, D. N. Basov, A. F. Starr, D. Schurig, and D. R. Smith, *Appl. Phys. Lett.* **88**, 081101 (2006).
- ⁷R. B. Greegor, C. G. Parazzoli, J. A. Nielsen, M. A. Thompson, M. H. Tanielian, and D. R. Smith, *Appl. Phys. Lett.* **87**, 091114 (2005).
- ⁸Q. Chen, *Plasmonics* **6**, 381 (2011).
- ⁹Y. Chen, C. Zhou, X. Luo, and C. Du, *Opt. Lett.* **33**, 753 (2008).
- ¹⁰X. M. Goh, L. Lin, and A. Roberts, *J. Opt. Soc. Am. B* **28**, 547 (2011).
- ¹¹A. K. Azad, A. J. Taylor, E. Smirnova, and J. F. O'Hara, *Appl. Phys. Lett.* **92**, 011119 (2008).
- ¹²W. J. Padilla, M. T. Aronsson, C. Highstrete, M. Lee, A. J. Taylor, and R. D. Averitt, *Phys. Rev. B* **75**, 041102 (2007).
- ¹³B. Scherger, C. Jördens, and M. Koch, *Opt. Express* **19**, 4528 (2011).
- ¹⁴Y. H. Fan, H. Ren, X. Liang, H. Wang, and S. T. Wu, *J. Disp. Technol.* **1**, 151 (2005).
- ¹⁵Y. Zhao, S. S. Lin, A. A. Nawaz, B. Kiraly, Q. Hao, Y. Liu, and T. J. Huang, *Opt. Express* **18**, 23458 (2010).
- ¹⁶X. Q. Lin, T. J. Cui, J. Y. Chin, X. M. Yang, Q. Cheng, and R. Liu, *Appl. Phys. Lett.* **92**, 131904 (2008).
- ¹⁷R. Liu, X. M. Yang, J. G. Gollub, J. J. Mock, T. J. Cui, and D. R. Smith, *Appl. Phys. Lett.* **94**, 073506 (2009).
- ¹⁸M. K. Chen, Y. C. Chang, C. E. Yang, Y. Guo, J. Mazurowski, S. Yin, P. Ruffin, C. Brantley, E. Edwards, and C. Luo, *Microwave Opt. Technol. Lett.* **52**, 979 (2010).
- ¹⁹M. D. Goldflam, T. Driscoll, B. Chapler, O. Khatib, N. M. Jokerst, S. Palit, D. R. Smith, B. Kim, G. Seo, H. Kim, M. Di Venira, and D. N. Basov, *Appl. Phys. Lett.* **99**, 044103 (2011).
- ²⁰I. V. Shadrivov, P. V. Kapitanova, S. I. Maslovski, and Y. S. Kivshar, *Phys. Rev. Lett.* **109**, 083902 (2012).
- ²¹I. E. Khodasevych, W. S. T. Rowe, and A. Mitchell, *Prog. Electromagn. Res. B* **38**, 57 (2012).
- ²²P. Ruffieux, T. Scharf, H. P. Herzig, R. Völkel, and K. J. Weible, *Opt. Express* **14**, 4687 (2006).
- ²³I. V. Shadrivov, A. B. Kozyrev, D. W. van der Weide, and Y. S. Kivshar, *Opt. Express* **16**, 20266 (2008).
- ²⁴I. E. Khodasevych, I. V. Shadrivov, D. A. Powell, W. S. T. Rowe, and A. Mitchell, in *APMC 2012 Conference* (2012), p. 451.
- ²⁵See supplementary material at <http://dx.doi.org/10.1063/1.4788918> for potentially useful operating regimes identified at other frequencies.